

Direct measurement of surface acoustic wave velocities and accuracy enhancement by wavelet transform

Klaus Kosbi, Ulla Scheer, Siegfried Boseck
Institute of Materials Science and Structure Research, Physics Department
University of Bremen, Kufsteiner Str., D-28359 Bremen, Germany

ABSTRACT

The aim of this work is to show that the wavelet transform as an image processing technique has the capability to improve quantitative measurements of surface acoustic wave (SAW) velocities. An outline of the basic properties of the wavelet transform and its advantages is given. We apply the wavelet transform to a recently developed measurement technique for the determination of SAW velocities. This technique is based on a modified scanning acoustic microscope (SAM) and can be thought as directly imaging SAWs that propagate on the surface of a solid. Results for the SAW velocity of silicon single crystals are presented.

INTRODUCTION

Scanning acoustic microscopy (SAM) is a useful technique to characterize solids in materials science. The principle of SAM is based on the reflection of ultrasound which is sensitive to the elastic properties of the specimen [1]. Therefore, a short radio frequency pulse is applied to a piezoelectric transducer so that mechanical vibrations are stimulated. These propagate as plane waves through the acoustic lens, usually a sapphire rod with its *c*-axis being the optical axis of the system. At its end the acoustic lens has a spherical calotte where the plane waves are refracted into converging spherical waves. Due to the difference in the acoustic impedances it is necessary to use a water droplet as a coupling fluid between the lens and the specimen. The focus is either adjusted onto the sample's surface (defocus $z = 0$) or inside the sample ($z < 0$) to image inner structures. After reflection the ultrasonic signal propagates the same way back to the transducer where now the piezoelectric crystal works as a receiver and converts the acoustic signal into an electrical output. By defocussing and increasing the aperture

angle of the lens bigger than a certain material dependent angle θ_R it is possible to stimulate surface acoustic waves (SAWs) that propagate on the sample's surface. By scanning the lens parallel to the specimen an image can be taken whereby the contrast arises from differences in the local impedance, stimulation of SAWs and the so called halo contrast around edges. In another mode of operation the lateral lens position is fixed and the output voltage V is measured as a function of the defocus z . From this so called $V(z)$ curve it is possible to derive the velocity of the SAWs [2] which is strongly dependent on the elastic constants of the investigated object. Our attention was concentrated on the development of an alternative method of measurement for the determination of those SAW velocities, because for ultrasonic frequencies higher than 0.5 GHz the $V(z)$ technique leads to measurement errors. For the SAM imaging mode we developed a new technique to determine SAW velocities with high accuracy at high frequencies [3]. The principle of this new method is described below. From the experimental setup it can be seen that the signal-to-noise ratio (SNR) decreases compared to conventional imaging with

SAM. In order to get more precise interpretation of our acoustical images we applied a digital image processing method using the wavelet transform and compared it with a conventional low pass filtering via FFT.

WAVELET THEORY AND DE-NOISING

The wavelet transform is a tool that expands data or functions into its components relative to a basis of translations and dilations of a so called mother wavelet $\psi(x)$. In traditional Fourier analysis a function is represented by a basis of constituent sinusoids of different frequencies. Via Fourier transformation one gets details about the frequency components in the given function while the locality information is lost. To correct this deficiency the short-time Fourier transform (STFT) was developed [4]. By windowing the function STFT maps it into a two-dimensional function of time and frequency. However, the precision of this method is determined by the size of the window and is hence strongly limited.

Wavelet analysis is more flexible than the STFT. It provides also a time-frequency description but with a few important differences. Any function which fulfills the admissibility condition

$$0 < c_\psi := 2\pi \int_{-\infty}^{\infty} \frac{|F_\psi(\omega)|^2}{|\omega|} d\omega < \infty$$

defines a wavelet. Mathematically the wavelet transform of a function $f(x)$ can be expressed as [5]:

$$L_\psi f(a, b) = \frac{1}{\sqrt{|a|}} \int_{-\infty}^{\infty} f(x) \psi\left(\frac{x-b}{a}\right) dx.$$

The so called daughter wavelets $\psi\left(\frac{x-b}{a}\right)$ are translated and dilated versions of $\psi(x)$ whereby a defines the dilation parameter (frequency) and b the translation parameter (localization). Compared to the STFT the daughter wavelets have localization-widths adapted to their frequency: high frequency daughter-wavelets $\psi^{a,b}$ are very narrow while low frequency $\psi^{a,b}$ are much broader. As a consequence, the wavelet transform can better 'zoom in' on very located high frequency phenomena, such as singularities and discontinuities in a function.

The formula given above can be generalized for higher dimensions. In case of two-dimensional data, e.g. an image, there are two possibilities for deriving the wavelet transform: one uses a two-dimensional wavelet for calculation and the other

consists of the realization of a one-dimensional transform on every dimension of the function.

In a wavelet decomposition of a signal or an image the wavelet coefficients correspond to details. Details that are small might be omitted without substantially affecting the main information. This is the idea of thresholding wavelet coefficients which is a way of cleaning out unimportant details considered to be noise. Thresholding generally gives a lowpass version of the original signal. There exist different methods how the data can be denoised. For the de-noising of our acoustical images we use a soft thresholding. For the image the wavelet coefficients d_{jk} are calculated. Soft thresholding shrinks all the coefficients towards the origin using a fixed threshold λ :

$$d_{jk} = \text{sign}(d_{jk})(|d_{jk}| - \lambda)$$

Afterwards the de-noised image is calculated from its wavelet coefficients via the inverse wavelet transform.

EXPERIMENT

The experimental setup for the direct imaging of SAWs is shown in fig.1. The acoustic lens is tilt-

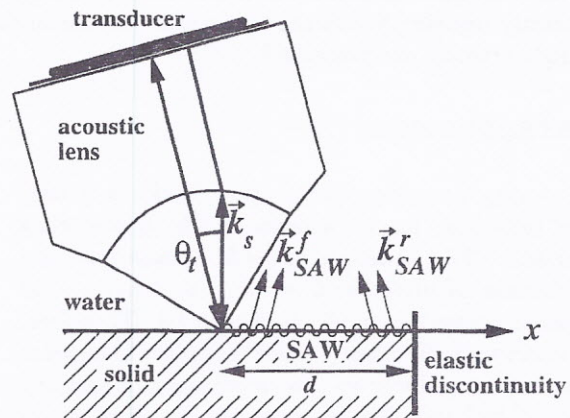


Fig. 1: Experimental setup for imaging interference fringes due to SAWs

ed by an angle θ_t that approximately equals the critical angle for stimulation of SAWs on the sample under investigation. The SAW propagates into x direction and leaks energy with wavevector \vec{k}_{SAW}^i back into the coupling medium. The SAW is then reflected at an elastic discontinuity and the reflected SAW leaks energy with wavevector \vec{k}_{SAW}^r into the coupling medium. The tilt angle θ_t

ensures maximum efficiency of stimulation of the forward propagating SAW and sensitivity for the reflected SAW. The transducer on the upper side of the acoustic lens measures the interference amplitude between the specularly reflected wave \vec{k}_s and the reflected SAW \vec{k}_{SAW}^r . While for a plane sample \vec{k}_s has constant phase, the phase of \vec{k}_{SAW}^r varies with the distance d between focus and the elastic discontinuity. Since the transducer detects the absolute value of the incoming amplitude, the output voltage in dependence on d shows oscillations with half the SAW wavelength. By scanning the lens parallel and perpendicular to the elastic discontinuity an image of the distribution of SAWs can be obtained (see fig. 2). The image analysis is done by calculating the Fourier transform of each column in the image and summing up the spectra to improve the SNR in the final spectrum.

RESULTS

Fig. 2 shows an image of horizontal equidistantly spaced interference fringes that are caused by SAWs propagating in [010] direction on a silicon Si(100) wafer. The reflecting elastic discontinuity is an etched structure of $1 \mu\text{m}$ height and does not lie within the scanned region of the image. The frequency that was used to stimulate the SAWs is 970 MHz and the lens was tilted by 17° which equals the Rayleigh angle of silicon. The broad vertical fringes in the image are an artifact that can be attributed to mechanical instabilities of the scanning system. Because of the high ultra-

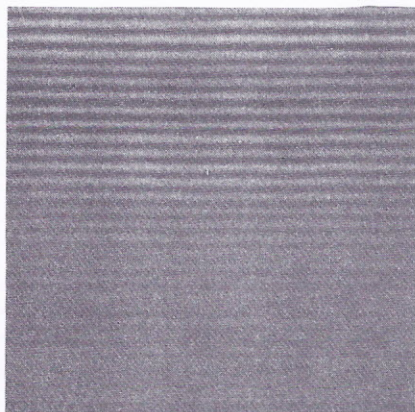


Fig. 2: Interference fringes caused by SAWs propagating in [010] direction on Si(100). Image width $75 \mu\text{m}$, frequency 970 MHz.

sound frequency the image is noisy. Two methods were used to improve the SNR in the im-

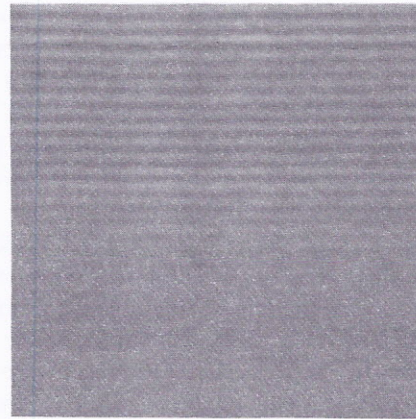


Fig. 3: Image of fig.2 after de-noising using Fourier low-pass filter.

age: first a Fourier low-pass filter and second a de-noising method based on a wavelet algorithm. Fig. 3 shows the image from fig. 2 after a Fourier low-pass filter operation. The image shows better contrast than the original data, but there is also a loss of resolution. Fig. 4 shows the de-noised image that was created by applying the wavelet algorithm to the original image. It can easily be seen that the image now shows more contrast and a highly improved SNR.

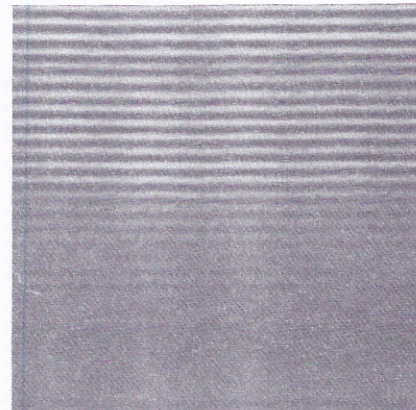


Fig. 4: Image of fig.2 after de-noising using a wavelet algorithm.

The one-dimensional Fourier powerspectra can be seen in fig. 5. The position of the main peaks that correspond to the periodicity of the SAW interference fringes rests fixed, so that the measured SAW velocity is not depending on the used image processing technique. In this case the SAW velocity was determined to be 4961 m/s which differs only by 0.8% from the literature value of 4921 m/s. The interesting fact is the drastical change in the height of the peaks: while Fourier

low-pass filtering decreases the spectral intensity compared with the original image, the spectrum of the wavelet transformed image shows a much higher peak. The different heights of the peaks correspond to different half widths of the peaks. So the highest peak for the wavelet transformed image shows the smallest half width.

In fig. 6. the three spectra are transformed so that the main peaks show the same relative height. So the SNR of the spectra can directly be compared. To make differences more clearly we present a logarithmic scaling of the spectral intensities. The interesting fact is, that the height of the spectral components in the low frequency region changes drastically: while Fourier low-pass filtering increases the spectral intensity compared with the original image, the spectrum of the wavelet transformed image shows slightly lower intensities for the low frequency noise.

We conclude that the wavelet transform is a well suited method for enhancement of imaged SAW interference pattern and improvement of measurement accuracy. It should also be possible to get SAW velocities of much worse images than that we presented here, for example when samples have higher values of SAW attenuation than silicon.

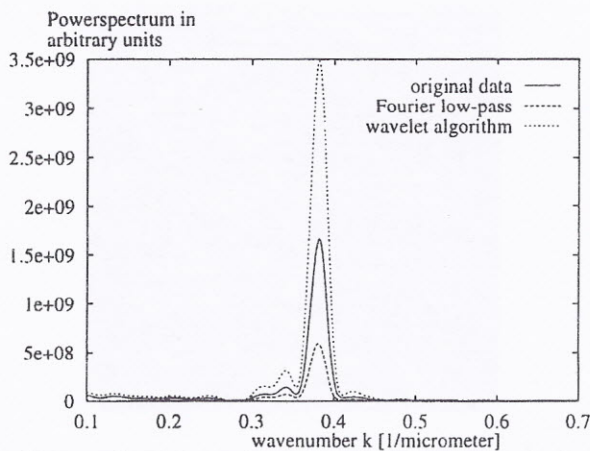


Fig. 5: One-dimensional Fourier transform of the images in fig. 2-4. $k = 2/\lambda_{SAW}$ is the spatial frequency of the interference fringes in the images and λ_{SAW} is the wavelength of the stimulated SAW.

SUMMARY

In this paper we presented the application of image processing techniques to a new measurement method of SAW velocities. This method makes use of the imaging mode of a scanning acoustic

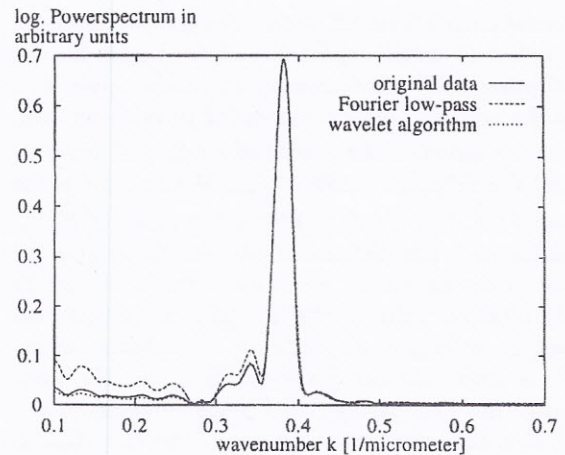


Fig. 6: Logarithmic representation of the one-dimensional Fourier transform of the spectrum in fig. 5

microscope. The images show interference fringes with spacings of half the SAW wavelength. As these images show only low contrast a method for enhancement of the measured intensities was desired. We found the wavelet algorithm to be a suitable image processing tool. While the SNR can slightly be improved, the measurement accuracy can be enhanced.

ACKNOWLEDGMENTS

This work is part of the doctor thesis of Ulla Scheer and Klaus Kosbi. We wish to thank the Deutsche Forschungsgemeinschaft (DFG) for its support (Bo 499/8-2).

REFERENCES

- [1] Briggs, A., 1992, Acoustic Microscopy, Clarendon Press, Oxford.
- [2] Weglein, R.D., 1985, Acoustic metrology, IEEE Trans. Sonics Ultrasonics SU-32, 225-234.
- [3] Kosbi, K., Weise, W., Scheer, U., Laun, U., Boseck, S., 1995, Measurement of surface wave velocity and anisotropy at edges using point-focus acoustic microscopy. In: Tortoli, P. (ed.), Proc. XXII Internat. Symposium on Acoustical Imaging, Plenum Press, 677-682.
- [4] Gabor, D., 1946, Theory of communication, J. IEE, Vol. 93, 429-455.
- [5] Daubechies, J., 1992, Ten Lectures on Wavelets, Academic Press, London.